ISSN 1062-8738, Bulletin of the Russian Academy of Sciences: Physics, 2022, Vol. 86, No. 8, pp. 948–955. © The Author(s), 2022. This article is an open access publication.
Russian Text © The Author(s), 2022, published in Izvestiya Rossiiskoi Akademii Nauk, Seriya Fizicheskaya, 2022, Vol. 86, No. 8, pp. 1146–1154.

New Technologies for the Vertex Detectors in the NICA Collider Experiments

V. I. Zherebchevsky[a], *, N. A. Maltsev[a], D. G. Nesterov[a], S. N. Belokurova[a], V. V. Vechernin[a], S. N. Igolkin[a], V. P. Kondratiev[a], T. V. Lazareva[a], N. A. Prokofiev[a], A. R. Rakhmatullina[a], and G. A. Feofilov[a]

[a] *St. Petersburg State University, St. Petersburg, 199034 Russia*

**e-mail: v.zherebchevsky@spbu.ru*

Received March 14, 2022; revised April 8, 2022; accepted April 22, 2022

Abstract—A review is presented of the latest technologies for vertex detectors that can be used in experiments at the NICA collider. These technologies include both the novel pixel detectors with new ultralight radiation-transparent carbon composite structures and cooling systems. The efficiency of reconstructing D meson decay is estimated for the developed detector complexes, and the possibility of using these complexes to study the formation of clusters of cold, dense quark-gluon matter inside nuclei are studied.

DOI: 10.3103/S1062873822080263

INTRODUCTION

Modern collider experiments with heavy ions in high-energy physics are aimed at studying phase transitions in strongly interacting matter. When relativistic heavy ions collide, quark–gluon matter can form in a deconfinement state: quark–gluon plasma (QGP), if the hadron system reaches a high density or temperature. The main scientific interest is to determine how does the transition of QGP to hadron gas occur. Experiments at the NICA collider under construction at the Joint Institute for Nuclear Research will give new information in this direction. One of these experiments calls the Multi-Purpose Detector (MPD). The aim of this experiment is to perform a detailed study of the phase diagram of nuclear matter in the region of high baryon density [1]. Such superdense matter could have existed at the early stages of the Universe evolution and might exist in the cores of neutron stars. No less interesting problems are encountered in the field of spin physics associated with the formation of the hadron spins, allowing for the spin and orbital moments of their constituent valence and sea quarks, along with gluons. Another experiment at the NICA collider, the Spin Physics Detector (SPD), is designed to cover these problems [2]. In both experiments, an important task is to study the yields of hadrons containing heavy quarks. Such hadrons are characterized by small cross sections of interaction with the nuclear medium and carry undistorted information about the states of nuclear matter that arise during the collision of relativistic nuclei. The effective extraction of charmed particles in events of nuclear–nuclear collisions detected by the experimental setup thus plays a key role in the analysis of possible phase transitions [3, 4].

The energy range of the NICA collider is $\sqrt{s_{NN}} = 4–11$ GeV for collisions of ^{197}Au(79+) ions with corresponding luminosities as high as 1×10^{27} cm^{-2} s^{-1} [5, 6]. The luminosity is several orders of magnitude higher for accelerated polarized protons and deuterons in the same range of energies: 1×10^{32} cm^{-2} s^{-1} [2]. It should be noted that collisions of heavy ions at the energies of the NICA collider are optimally suited to create a high baryon density and achieve the deconfinement phase of nuclear matter. This will allow us to study the properties of a superdense nuclear medium, including the search of deconfinement signals and a critical point on the phase diagram.

Theoretical studies and the experimental information available today show that an increased yield of hadrons containing strange and charmed quarks is observed during the formation of QGP. The same particles also occur in collisions between relativistic beams of polarized protons and deuterons. The origin processes of such hadrons (e.g., hyperons and charmed mesons) are quite rare. To detect these particles, the new detector technologies with minimal noise and high time, energy, and radiation characteristics sould be used. On the other hand, the multiplicity of the secondary particles generated in the central collisions of relativistic ions can be as high as several thousand in the energy range of the NICA collider. For reliable registration of such events, we need detectors that are capable of reconstructing tracks of primary charged particles and their decay products with

high efficiency. Tracking systems that allow us to reconstruct the decay vertices of short-lived hadrons must have high spatial resolution. To create such systems, the technologies of silicon pixel detectors based on CMOS (used today in high-energy physics experiments [7–11]) should be applied.

At the relatively low energies of colliding nuclei at the NICA collider ($\sqrt{s_{NN}}$ = 4–11 GeV), it becomes possible to study various clusters of dense nuclear matter inside them [3, 4]. One sign of the existence of such clusters is the formation of particles during scattering on nuclei in areas kinematically forbidden for reactions with free nucleons, which is usually referred to as cumulative generation. In this work, we discuss technologies for creating vertex detectors in experiments at the NICA collider. The novel silicon pixel detector complexes are considered with ultralight radiation-transparent carbon composite structures for their support, and with efficient cooling systems for these detector complexes.

MODERN VERTEX DETECTORS IN COLLIDER EXPERIMENTS

Tracking systems are widely used today to provide experimental research in the field of high-energy physics and elementary particles physics. One of the main modules of such tracking systems is a vertex detector designed for precisely determination of short lived hadrons decay vertices, using the reconstructed tracks of their decay products. In experiments on fixed targets, the vertex detectors are usually located almost immediately behind a target covering a wide solid angle of the detected particles. In collider experiments, the vertex detector is mounted close to the interaction point. They are usually placed inside the main tracking system. A time-projection chamber is such a system in several experiments. To detect hadrons originated in reactions with relativistic heavy ions and subsequently identify their tracks and the tracks of decay products of unstable hadrons, we need accurately determine the coordinates of the primary vertex and the secondary vertices. Intensive research on new silicon coordinate-sensitive pixel detectors with both high spatial resolution and high counting rate is currently under way.

The work of the Large Hadron Collider (LHC) at CERN and the ALICE experiment (A Large Ion Collider Experiment) have allowed us to study the phase diagrams of strongly interacting matter at high temperatures. It became possible to analyze several characteristics of QGP, the properties of which were studied earlier in experiments on collisions of relativistic heavy ions at the SPS (CERN) and RHIC (BNL) accelerators. On the other hand, measurements of the yields of particles with heavy flavours (particles containing c and b quarks) with increased luminosity of the LHC in 2022 in the collisions of lead ions up to 6×10^{27} cm^{-2} s^{-1} will allow us to determine such parameters of strongly interacting matter as the initial temperature of QGP and study different dynamic processes in a QGP medium [9]. Detecting particles containing heavy flavours one can answer questions about thermalization and hadronization of QGP (heavy flavours carry information about the state of the medium at the time of their origination). To obtain a complete physical picture of the events of nuclear–nuclear collisions, the efficiency of detected particle track identification, especially in the region of low transverse momenta should be improved. The spatial resolution for identification of the primary and secondary vertices of charmed and beauty hadrons also has to be improved. Registering events at the increased luminosity of the LHC requires the development of new technologies to create high-count rate detector systems. Monolithic Active Pixel Sensors (MAPS) based on CMOS technology (180 nm) are such new detector systems. An important advantage of these pixel detectors over the currently used hybrid pixel detectors is that all detector electronics (amplifier, discriminator, memory buffer) are placed on a single chip and integrated directly into the sensor. Each pixel is one detector. Over the past 30 years, intensive applied research has been done on detectors based on CMOS technologies to use them for detecting charged particles [12–15]. It is now possible to design and create vertex detectors for experiments in elementary particle and nuclear physics [10, 11, 16–19]. The first such detector using CMOS-based sensors was used in the STAR (Solenoidal Tracker At RHIC) experiments at the Relativistic Heavy Ion Collader RHIC [12, 20]. It was possible to identified the processes of the origin of lambda hyperons containing heavy flavours (c-quarks) in collisions between gold ions at energy $\sqrt{s_{NN}}$ = 200 GeV [21]. However, the CMOS technologies (350 nm technology) used in these pixel sensors cannot be implemented for several parameters at the upgraded ITS of the ALICE experiment at the LHC or for creating new vertex detectors at the NICA collider. Since such detectors cannot be used in high intensity collisions because of the short time to read information from pixels (320 Mbit/s), the long time of signal integration (190 microseconds), and the significant power density on the detector modules (up to 150 mW cm^{-2}). These limitations can be overcome if 180 nm technology is used. The new ITS of the ALICE experiment uses the ALPIDE pixel CMOS detectors [8], which have an information readout time of 1200 Mbit/s and an period of integration of 4 microseconds. These detectors have rather low power density (about 40 mW cm^{-2}), high spatial resolution (5 μm), and good radiation tolerance. Four generations of such detectors have been developed, and the comprehensive studies of their properties have been performed [22–24]. Results have answered several technological questions and allowed to create a working ALICE tracking system based on

MAPS [7]. Information from studies of the characteristics of such pixel detectors and their identification ability when detecting short-range particles and their decay products have led to the concept of a vertex detector for the Mega-project Multi-Purpose Detector at the NICA collider [3]. Comprehensive analysis of data obtained by irradiating detectors (in a telescope configuration) with different types of radioactive sources (gamma, beta, alpha) and high-energy electrons (on a linear accelerator), along with experiments using this telescope to detect cosmic ray particles, has contributed to the improvement of detection systems and data processing algorithms for the vertex detectors based on the latest pixel sensors for experimental setups of the NICA complex.

In creating modern vertex detectors for the collider experiments, it should be considered that when registering the hadrons containing heavy quarks and their decay products, the trajectories of such particles should not deviate much from the original direction due to multiple scattering on the materials and structural elements of the detectors. Therefore a detector system with great radiation transparency should be built. The supporting structures that make up the detector modules and their cooling systems should have a minimum of matter with the minimum thickness of the silicon detectors [25, 26]. Record values of radiation transparency with a minimum material budget in mega-detectors in the high energy physics (at a level of 0.39% for a layer of silicon detectors) have been achieved for the new inner tracking system of the ALICE experiment at the LHC at CERN [8]. A similar concept is being used to create a vertex detector (VD) for the MPD experiment at the NICA collider. The pixel detectors will be mounted on ultralight carbon composite support structures with an integrated cooling system. These structures will be combined into ladders along the surface of coaxial cylinders around the interaction points of the NICA collider beams. Modeling and calculations have shown that for reliable reconstruction of the decay vertices of short-lived particles, the radiation thickness of the detectors (including cable systems and detector support structures) should not be more than 1% of the charged particle radiation length. This is necessary to reduce the effect of multiple scattering which can make change the VD spatial resolution. The detector ladders (with corresponding ultralight carbon composite structures) forming cylindrical layers around the interaction point of NICA collider beams will partially overlap to exclude the formation of dead zones throughout the VD working volume. Note that the minimum distance between cylindrical layers, which is determined by the size of the carbon-composite structures, is also considered when determining their number. The complete concept of the VD was presented in [3, 4], which also outlined the tasks of manufacturing and studying the physical, structural, and functional features of ultralight radiation-transparent carbon composite structures for supporting detectors based on MAPS. A prepreg consisting of high-modulus carbon fiber with an appropriate binder agent is used on the design of these support structures. The combination of these components allows us to obtain detector support structures with the best mechanical properties. In creating support structures for detectors based on MAPS for the MPD experiment, wound-truss structures of 1526 mm long were developed using a prepreg of russian production (NIIKAM-RS/M55). To determine the parameters of such a prepreg, efforts were made to identify the actual amount of fiber in it. It was found that this prepreg differs from the foreign analogs with less carbon fiber and more epoxy binder agent. A low content of carbon fiber can result in deterioration of the supporting structure strength, since the main parameter of a wound-truss structure is its rigidity, which is determined by the shape of the product, and the modulus of the material and its quantity. Several samples of ultralight carbon composite structures for supporting MAPS detectors were therefore made and their geometric, mechanical, and strength properties were studied to compare the obtained data with characteristics of ultralight carbon composite structures for the ALICE experiment at the LHC. It turned out that the geometric characteristics of the support structures were identical (within the measuring error), but the ALICE wound-truss structures were heavier and more rigid: deviation was no more than 0.20 mm with a central load of 200 *g*. Such differences between the characteristics of carbon support structures were due to the properties of our prepreg containing less carbon fiber. This makes the manufactured product lighter and reduces its rigidity. Our studies have shown that even a small difference in the content of carbon fiber in the prepreg (~20%) substantially affects the mechanical and geometric properties of ultralight carbon composite support structures. We therefore decided to modify the technology of producing these support structures to create a vertex detector for the MPD experiment: the number of prepreg layers was raised to nine, and bundles of three carbon fibers were laid on the edges of the wound-truss structures. The manufactured support structures (see Fig. 1) thus began to match those of ALICE in terms of their mechanical and strength characteristics. In the future, in collaboration with the Joint Institute of Nuclear Research, the carbon fiber panels with an integrated liquid cooling system will be mounted on these wound-truss structures with monolithic active pixel detectors.

RECONSTRUCTING OF D MESON DECAYS IN THE MPD EXPERIMENT'S TRACKING SYSTEM AT THE NICA COLLIDER

Model estimates of the efficiency of reconstructing D meson decays in the MPD experiment's tracking system at the NICA collider were made on the basis of

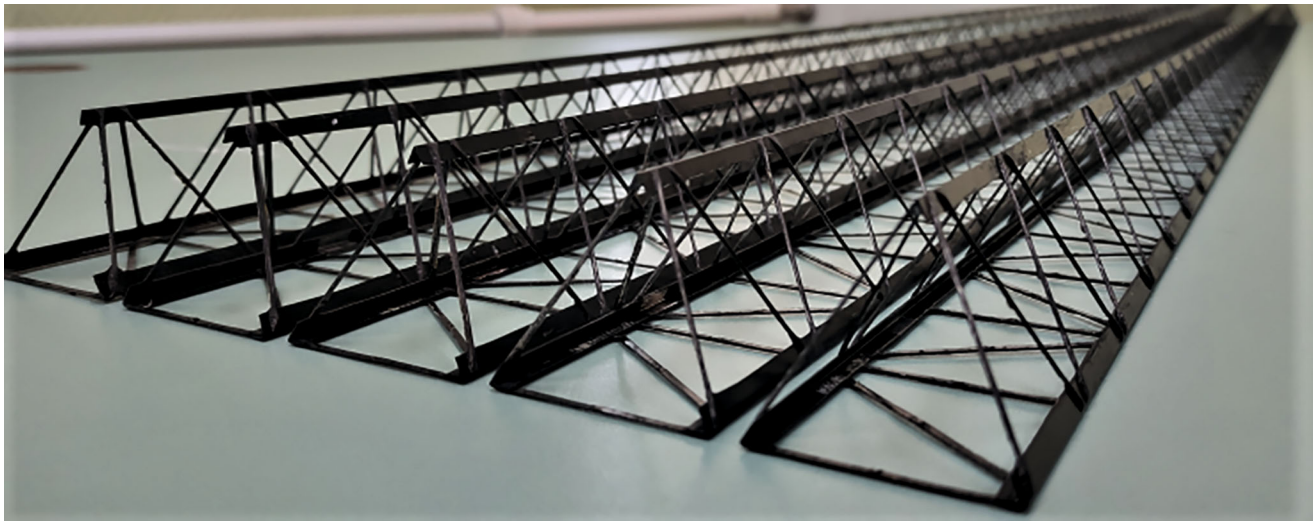

Fig. 1. The wound-truss ultralight carbon composite structures for detector systems based on MAPS.

the functionality and characteristics of monolithic active pixel sensors discussed above.

A time-projection chamber (TPC) is the main tracking detector in the MPD experiment. The TPC will provide reconstruction of charge particle tracks in the central region of rapidities, along with their identification by measured energy losses [27]. For reliable identification of short-lived hadrons (which include charmed mesons), the TPC will be supplemented with a vertex detector. As already noted, the MPD experiment VD will consist of MAPSs combined into ladders located along the surface of the coaxial cylinders around the interaction point of the NICA collider beams. A five-layer design of the VD, adapted for the beam pipe of the NICA collider with a diameter of 40 mm (VD5-40), was proposed in [3]. It was shown that using such a VD provides spatial resolution sufficient for reconstructing the decays of unstable particles, the average ranges λ of which are several hundred micrometers [3].

The identification capability of the MPD experiment tracking system consisting of the TPC and VD5-40 was evaluated by reconstructing decay vertices D^0 ($\lambda = 123$ μm) and D^+ ($\lambda = 312$ μm) formed in central Au + Au collisions at energy $\sqrt{s_{NN}} = 9$ GeV. The decays of D^0 and D^+ mesons was reconstructed in the Mpdroot object-oriented software environment [28]. Nucleus–nucleus collisions were emulated on the basis of a QGSM event generator built using the quark–gluon string model [29]. Pure signal events corresponding to the decays of charmed mesons were played out using a thermal generator [30] tuned to the energy of the NICA collider. In events of nucleus–nucleus collisions, the background for the signals corresponding to the decays of the short-lived particles was a large number of random combinations of tracks that did not correspond to the true products of a particle's decay. Considerable suppression of such a combinatorial background can be achieved using the criteria for selecting useful events according to such topological parameters as the distance of the closest approach between the decay-product tracks and the primary vertex of the colliding nuclei interaction (*dca*); the distance between the tracks of daughter particles at the decay vertex of the parent particle (*distance*); the length of the path of the parent particle from its point of formation to the point of decay (*path*); and the angle between the vector connecting the primary and secondary vertices and that of the reconstructed momentum of the parent particle (*angle*). The values of the specified selection parameters (cuts) for each type of particle were selected according to the maximum of significance function Sign(a) for each parameter a:

$$\mathrm{Sign}(a) = \int_0^a \frac{S(a')}{\sqrt{S(a') + B(a')}} da',$$

where $S(a)$ and $B(a)$ are the distribution of signal and background events according to parameter a. D mesons were identified by selecting the peak corresponding to the parent particle in the invariant mass spectrum of its decay products along a fixed hadron channel. Table 1 shows the decay channels of the D^0 and D^+ mesons, with evaluated efficiency of their reconstruction.

To extract D^0 and D^+ signals, we processed 10^6 signal events $D^0 \to K^- + \pi^+$ and $D^+ \to K^- + \pi^+ + \pi^+$ and 10^5 events of the central Au + Au collisions. When reconstructing the decay vertex of D mesons, only the tracks of products of their decay that were reconstructed using the responses of pixel detectors in all 5 layers of the VD. To reduce the combinatorial background, we selected *dca* cuts at the level of 2σ of the

Table 1. D^0 and D^+ decay channels used for their reconstructing in the MPD experiment tracking system

Адрон	Mass, MeV s^{-2}	cτ, μm	Decay channel	Branching ratio, %
D^+	1869.62 ± 0.20	312	$\pi^+ + \pi^+ + K^-$	9.13
D^0	1864.84 ± 0.17	123	$\pi^+ + K^-$	3.89

width of their distributions were selected. The cut values were applied to the signal and background events. The signal invariant mass spectrum satisfying the choisen selection criteria was reduced to statistics of 10^8 central Au + Au collisions, considering the multiplicity of D mesons and the probability of their decay along a fixed channel (see Table 1). The multiplicity of D mesons in the central Au + Au collisions was estimated using the dynamic model of a hadron string [31] and was 10^{-2} meson/event at the energies of the NICA collider. The combinatorial background remaining after applying the cuts was uniformly distributed over the selected range by the invariant mass and then reduced to statistics of 10^8 events with the addition of statistical fluctuations. Figure 2 shows the resulting spectra for D^0 (Fig. 2a) and D^+ (Fig. 2b) obtained by summing the signal and background spectra normalized to 10^8 central Au + Au collisions. Analysis of the distributions depicted in Fig. 2 showed that signals can be selected on a combinatorial background with such statistics at significance levels of 5.3 for D^0 and 7.0 for D^+, and the efficiency of reconstructing D^0 and D^+ mesons was 0.8 and 0.5%, respectively.

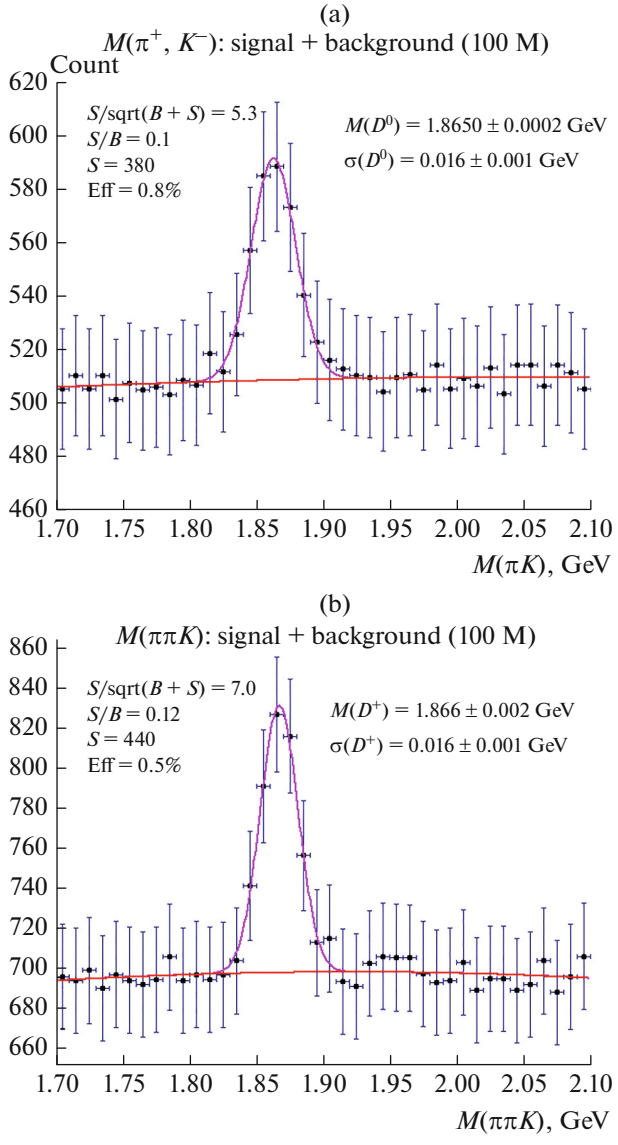

Fig. 2. (a) D^0 and (b) D^+ signals in the invariant mass spectrum extracted in 10^8 central Au + Au collisions at energy $\sqrt{s_{NN}}$ = 9 GeV: full spectrum (purple line) and residual combinatorial background (red line).

VERTEX DETECTORS FOR CUMULATIVE PROCESSES STUDYNG

Important problems that can be investigated experimentally in the MPD and SPD experiments at the NICA collider are detecting and studying the properties of clusters of dense cold nuclear matter ("fluctuons") that can spontaneously arise in colliding nuclei [32]. Modern models interpret such a multi-nucleon cluster as a state in which all quarks and gluons of the nucleons contained in it are in a state of deconfinement at zero temperature and high baryon density (cold quark–gluon plasma). Experimental studies of such new states of matter at the NICA collider are of great physical interest. A consequence of fluctuons being in colliding nuclei is the possible formation of particles with momenta lying outside the kinematic region allowed for single nucleon-nucleon collisions (in the so-called cumulative region) [33–36]. From an experimental point of view, we can study such cumulative generation in collider experiments only at relatively low initial energies (preferably at energy $\sqrt{s_{NN}}$ = 4 GeV at the NICA collider) [3, 37], since it is impossible in experiments at high energies at the RHIC and LHC colliders. Therefore it is needed to perform experiments at the NICA collider to study clusters of cold dense quark–gluon matter in nuclei. Since there are currently numerous alternative models of particle formation in the cumulative region [38–41], to select and confirm the flucton mechanism of particle forma-

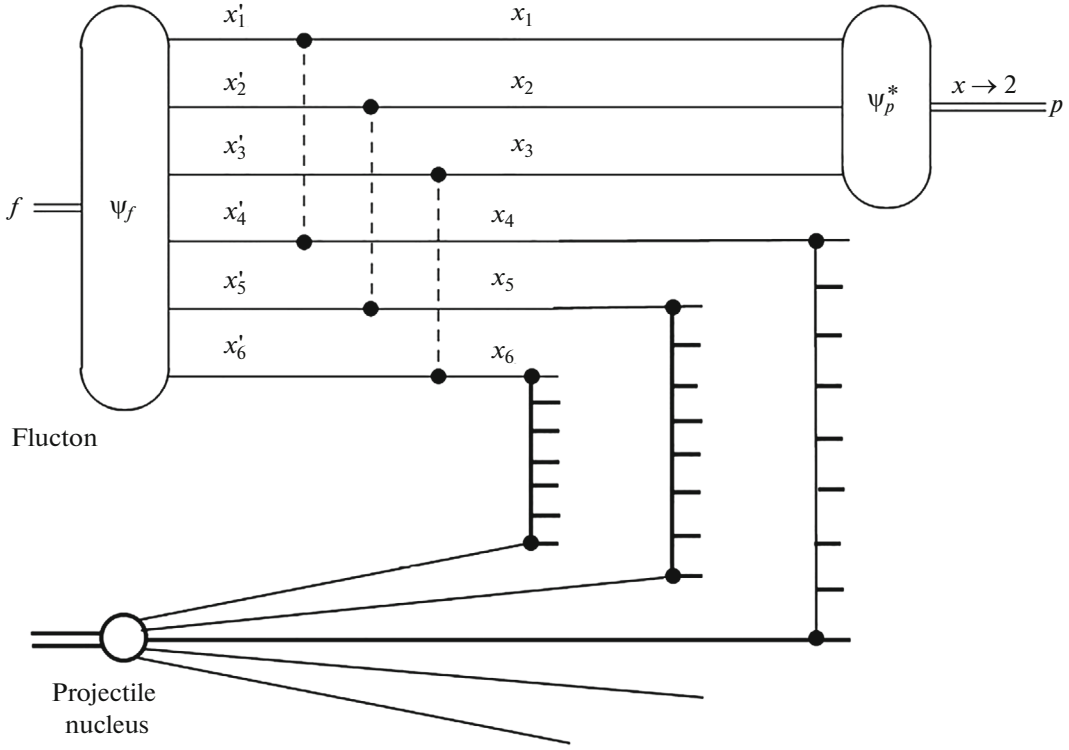

Fig. 3. Interaction between a two-nucleon flucton ($6q$) of one nucleus with partons of another nucleus [46, 48]. The dotted ladders show the exchanges of hard gluons [41].

tion in this region, one can need to detect with cumulative particles, all particles formed during the fragmentation of flucton residue [42, 43]. As the theoretical analysis [44–47] showed, the mechanisms of the formation of cumulative protons and pions within the flucton model also differ. When the formation of pions occurs due to fragmentation into a pion of one of the flucton quark [44], the main contribution to the origin of cumulative protons comes from the mechanism of coherent coalescence (recombination) of three flucton quarks into a proton [45–47] (see diagram in Fig. 3). Figure 3 shows the formation of cumulative protons by coherent coalescence (recombination) of three flucton quarks, while (as shown by our analysis of the fragmentation of fluctons in the cumulative region [46]) the contribution from Feynman diagrams, in which all the remaining flucton quarks interact with the partons of the incoming nucleus, predominates. Quark–gluon strings form when these remaining quarks of the fluctuon interact with the partons of an incoming nucleus. Since a flucton is a compressed configuration in the transverse plane and otherwise, the resulting strings appear to overlap in the plane of the impact parameter. In this case, it is possible to merge these strings into string clusters (so-called "color ropes") [49, 50]. The formation of such fused strings with increased strain (increased intensity of the color field) increases the yields of particles with heavy quarks [51, 52]. This process at the energies of the NICA collider will increase the yields of strange particles [48] in the kinematic region where particles originate during the fragmentation of flucton residue.

Therefore we need together with cumulative particles to detect all particles that form during the fragmentation of flucton residue in order to confirm the existence of clusters of cold dense quark–gluon matter in nuclei and study the details of the mechanism of particle formation in the cumulative region with their participation. Since the formation of the cumulative particles is a rare phenomenon, their study requires experiments at the maximum possible luminosity of the NICA collider. The problem of excluding the influence of so-called "pile-up" effects on experimental results then arises. A vertex detector with high spatial resolution should be used to exclude all tracks of particles emerging from the vertices of other collisions (which can be near the vertex of the main collision) in which a cumulative particle forms. Leaving such tracks would distort the spectrum of particles originating from the fragmentation of the flucton residue, studies of which are of great physical interest. With increased luminosity $\sim 10^{30}$ cm^{-2} s^{-1} of the NICA collider for Au + Au collisions, the probabilities of having other vertices of Au + Au interaction at distances of less than 0.5 and 0.1 mm are 0.18 and 0.037%, respectively [38]. This demonstrates the need to use a vertex detector in MPD or SPD experiments to suppress the contribu-

tion from pile-up effects when recording the spectrum of the particles that form because of the fragmentation of flucton residue.

CONCLUSIONS

A brief overview about novel vertex detector for collider experiments was presented. It was shown that thin Monolithic Active Pixel Detectors with high spatial resolution and high counting rate can serve as the main modules for creating vertex detectors. Studies of carbon composite materials and new technologies to design ultralight support structures for such pixel detectors also were included in this report. It was shown that the developed support structures in their geometric, mechanical, and strength values have the similar characteristics like ultralight carbon composite support structures for the MAPS detectors used in the ALICE experiment at the LHC.

As theoretical investigations the model estimations of the reconstructing efficiency of D mesons decays using the vertex detector of the MPD experiment were done. The estimates showed that the signal selection on a combinatorial background can be performed at significance levels of 5.3 and 7.0 for D^0 and D^+, respectively, and the efficiency of reconstructing D^0 and D^+ mesons approaches is about 1%.

New physical phenomena associated with the existence of cold dense clusters of quark–gluon matter in nuclei with the formation of particles in the cumulative region have been studied. It was shown that we need to detect both cumulative particles and ones that form during the fragmentation of flucton residue. It was proposed that a vertex detector with high spatial resolution in collider experiments should be used to suppress pile-up effects that can mix the tracks of particles from different vertices.

FUNDING

This work was supported by the Russian Foundation for Basic Research, project no. 18-02-40075.

CONFLICT OF INTEREST

The authors declare that they have no conflicts of interest.

OPEN ACCESS

REFERENCES

1. Nuclotron-based Ion Collider fAcility (NICA). https://nica.jinr.ru/projects/mpd.php.
2. Spin Physics Detector. http://spd.jinr.ru/spd-cdr.
3. Zherebchevsky, V.I., Kondratiev, V.P., Vechernin, V.V., and Igolkin, S.N., *Nucl. Instrum. Methods Phys. Res., Sect. A*, 2021, vol. 985, 164668.
4. Zherebchevsky, V.I., Vechernin, V.V., Igolkin, S.N., et al., *Bull. Russ. Acad. Sci.: Phys.*, 2021, vol. 85, p. 541.
5. Kekelidze, V., Kovalenko, A., Lednicky, R., et al., *Nucl. Phys. A*, 2017, vol. 967, p. 884.
6. Kekelidze, V.D., Matveev, V.A., Meshkov, I.N., et al., *Phys. Part. Nucl.*, 2017, vol. 48, no. 5, p. 727.
7. CERN Courier. https://cerncourier.com/a/alice-tracks-new-territory.
8. Abelev, B., Adam, J., Adamová, D., et al, *J. Phys. G*, 2014, vol. 41, 087002.
9. Bevan, A., Crooks, J., Turchetta, R., et al., *Nucl. Instrum. Methods Phys. Res., Sect. A*, 2011, vol. 643, no. 1, p. 29.
10. Wang, T., Barbero, M., Berdalovic, I., et al., *J. Instrum.*, 2018, vol. 13, no. 3.
11. Contin, G., Greiner, L., Schambach, J., et al., *Nucl. Instrum. Methods Phys. Res., Sect. A*, 2018, vol. 907, p. 60.
12. Turchetta, R., Berst, J.D., Casadei, B., et al., *Nucl. Instrum. Methods Phys. Res., Sect. A*, 2014, vol. 458, p. 677.
13. Ballin, J., Coath, R., Crooks, J., et al., *J. Instrum.*, 2011, vol. 6, P05009.
14. McMullan, G., Turchetta, R., and Faruqi, A.R., *J. Instrum.*, 2011, vol. 6, C04001.
15. Peric, I. and Berger, N., *Nucl. Phys. News*, 2018, vol. 28, no. 1, p. 25.
16. Terzo, S., Cavallaro, E., Casanova, R., et al., *J. Instrum.*, 2017, vol. 12, no. 6, C06009.
17. Aglieri Rinella, G. (on behalf of the ALICE Collab.)., *Nucl. Instrum. Methods Phys. Res., Sect. A*, 2017, vol. 845, p. 583.
18. Koziel, M., Amar-Youcef, S., Bialas, N., et al., *Nucl. Instrum. Methods Phys. Res., Sect. A*, 2017, vol. 845, p. 110.
19. Besson, A., Perez, A.P., Spiriti, E., et al., *Nucl. Instrum. Methods Phys. Res., Sect. A*, 2017, vol. 845, p. 33.
20. Contin, G., *Nucl. Instrum. Methods Phys. Res., Sect. A*, 2016, vol. 831, p. 7.
21. Xie, G. (for the STAR Collab.), *Nucl. Phys. A*, 2019. https://arxiv.org/pdf/1704.04353.pdf.
22. Mager, M., (on behalf of the ALICE Collab.), *Nucl. Instrum. Methods Phys. Res., Sect. A*, 2016, vol. 824, p. 434.
23. Zherebchevsky, V.I., Kondratiev, V.P., Krymov, E.B., et al., *Bull. Russ. Acad. Sci.: Phys.*, 2016, vol. 80, no. 8, p. 953.

24. Yang, P., Aglieri, G., Cavicchioli, C., et al., *JINST*, 2015, vol. 10, C03030.
25. Zherebchevsky, V.I., Altsybeev, I.G., Feofilov, G.A., et al., *J. Instrum.*, 2018, vol. 13, T08003.
26. Zherebchevsky, V.I., Igolkin, S.N., Krymov, E.B., et al., *Instrum. Exp. Tech.*, 2014, vol. 57, no. 3, p. 356.
27. Abraamyan, Kh.U., Afanasiev, S.V., Alfeev, V.S., et al., *Nucl. Instrum. Methods Phys. Res., Sect. A*, 2011, vol. 628, p. 99.
28. GitLab. http://git.jinr.ru/nica/mpdroot.
29. Gudima, K.K., Mashnik, S.G., and Sierk, A.J., Report LA-UR-01-6804, Los Alamos, 2001.
30. Tawfik, A.N. and Abbas, E., *Phys. Part. Nucl. Lett.*, 2015, vol. 12, p. 521.
31. Cassing, W., Bratkovskaya, E.L., and Sibirtsev, A., *Nucl. Phys. A*, 2001, vol. 691, p. 753.
32. Blokhintsev, D.I., *Zh. Eksp. Teor. Fiz.*, 1957, vol. 33, p. 1295.
33. Leksin, G.A., et al., *Zh. Eksp. Teor. Fiz.*, 1957, vol. 32, p. 445.
34. Baldin, A.M., *Yad. Fiz.*, 1973, vol. 18, p. 79.
35. Efremov, A.V., *Fiz. Elem. Chastits At. Yadra*, 1982, vol. 13, no. 3, p. 613.
36. Burov, V.V., Lukyanov, V.K., and Titov, A.I., *Phys. Lett. B*, 1977, vol. 67, p. 46.
37. Vechernin, V.V., *Phys. Part. Nucl.*, 2021, vol. 52, no. 4, p. 604.
38. Frankfurt, L.L. and Strikmann, M.I., *Phys. Rep.*, 1981, vol. 76, p. 215.
39. Motornenko, A. and Gorenstein, M.I., *J. Phys. G*, 2017, vol. 44, 025105.
40. Efremov, A.V., Kaidalov, A.B., Kim, V.T., et al., *Yad. Fiz.*, 1988, vol. 47, p. 1364.
41. Braun, M.A. and Vechernin, V.V., *Nucl. Phys. B*, 1994, vol. 427, p. 614.
42. Stavinskiy, A., *Phys. Part. Nucl. Lett.*, 2011, vol. 8, no. 9, p. 912.
43. Stavinskiy, A., *EPJ Web Conf.*, 2014, vol. 71, 00125.
44. Braun, M.A. and Vechernin, V.V., *Phys. At. Nucl.*, 2000, vol. 63, p. 1831.
45. Braun, M.A. and Vechernin, V.V., *Nucl. Phys. B, Proc. Suppl.*, 2001, vol. 92, p. 156.
46. Braun, M.A. and Vechernin, V.V., *Theor. Math. Phys.*, 2004, vol. 139, p. 766.
47. Vechernin, V.V., *AIP Conf. Proc.*, 2016, vol. 1701, 060020.
48. Vechernin, V.V., *Proc. Int. Conf. on Strangeness in Quark Matter 2019*, Bari, 2019.
49. Braun, M.A. and Pajares, C., *Nucl. Phys. B*, 1993, vol. 390, p. 542.
50. Vechernin, V.V. and Belokurova, S.N., *J. Phys.: Conf. Ser.*, 2020, vol. 1690, 012088.
51. Armesto, N., Braun, M.A., Ferreiro, E.G., and Pajares, C., *Phys. Lett. B*, 1995, vol. 344, p. 301.
52. Ferreiro, E.G. and Pajares, C., *J. Phys. G*, 1997, vol. 23, p. 1961.

Translated by N. Petrov